NASA-CR-191267

ABSOLUTE ABSORPTION CROSS SECTIONS OF OZONE AT 300 K, 228 K AND 195 K IN THE WAVELENGTH REGION 185-240 nm

Grant NAGW-1788

Final Report

For the period 1 June 1989 through 31 May 1992

Principal Investigator
K. Yoshino

Co-Investigators
W.H. Parkinson
D.E. Freeman

September 1992

Prepared for
National Aeronautics and Space Administration
Greenbelt, Maryland 20771

Smithsonian Institution
Astrophysical Observatory
Cambridge, MA 02138

The Smithsonian Astrophysical Observatory
is a member of the
Harvard-Smithsonian Center for Astrophysics

The NASA Technical Officer for this grant is Dr. Igor J. Eberstein,
Code 616, Goddard Space Flight Center, Greenbelt, Maryland 20771.

Abstract

An account is given of progress during the period 10/1/89-5/31/92 of work on absorption cross section measurements of ozone at 300 K, 228 K and 196 K in the wavelength region 185-240 nm. In this wavelength region, the penetration of solar radiation into the Earth's atmosphere is controlled by O_2 and O_3. The transmitted radiation is available to dissociate trace species such as halocarbons and nitrous oxide. We have recently measured absolute absorption cross sections of O_3 in the wavelength region 240-350 nm [Freeman et al., 1985; Yoshino et al., 1988]. We apply these proven techniques to the determination of the absorption cross section of O_3 at 300 K, 228 K and 195 K throughout the wavelength region 185-240 nm. A paper titled "Absolute Absorption Cross Section Measurements of Ozone in the Wavelength Region 185-254 nm and the Temperature Dependence" has been submitted for publication in the Journal of Geophysical Research.

1. FINAL REPORT FOR THE PERIOD 1/10/89-5/31/92

1.1. The absolute absorption cross section of ozone

The absolute absorption cross section of ozone at fixed wavelengths in the region 184-245 nm have been measured at 295, 228 and 195 K. The fixed wavelengths have been selected from atomic lines of Hg I, Cu I and Cu II. The mercury lamp with thermal control and a special Cu hollow cathode lamp provide suitable atomic line sources. The absorption cross section of ozone in the wavelength region 185-250 nm varies from 1.15×10^{-17} to 3×10^{-19} cm^2. The optical depths measured were restricted to the range $\ln(I_0/I) \simeq$ 0.3-2.0 to ensure good accuracy. With this restriction, the whole set of cross section measurements can be performed with pressures of O_3 in the range 0.1-11 Torr.

The vacuum system must be completely free from any contaminants which might destroy ozone. After the vacuum system is baked, ozone is stored for days to "clean up" the vacuum system. Ozone is prepared from pure oxygen (Airco grade 4.5 passed through a liquid nitrogen trap) at 78 K in a Tesla discharge, collected as liquid ozone at 78 K, and purified of residual oxygen from the oxygen/ozone mixture at 78 K.

Experimental conditions are summarized in Table 1 where the number of measurements (n), the electric current in hollow cathode lamp (I), and counting time (T) are listed. The absolute absorption cross sections of ozone have been measured at 12 wavelengths throughout the region 184—245 nm at 295, 228 and 195 K. The results are listed in Table 2, where values from Molina and Molina are presented in 6th and 7th column and they are slightly higher than our present values. Absolute cross section measurements at five mercury wavelengths (253.6-334.1 nm) from seven independent workers (see Table 2 of Yoshino et al., 1988) are scattered within 2.5% of the averaged values but the values by Molina and Molina (1986) were slightly higher than other measurements.

1.2. The cross sections of ozone in the wavelength region 180-245 nm

Continuous cross sections of ozone were measured in the wavelength region 180—245 nm with a hydrogen continuum as background source. A mercury lamp was also placed behind the hydrogen lamp and provided two Hg lines at 184.9 and 253.7 nm. These two Hg lines were used for wavelength calibration. The column density of ozone is expected to vary during the scanning of the entire wavelength region because the vuv radiation destroys ozone molecules. However the scan over an extended wavelength region is used to provide only continuous relative cross sections.

Table 1. Experimental conditions for the absolute cross section measurements of ozone at fixed wavelengths

295K

λ nm	n	Line	I mA	T Sec	Slit μm	Pressure Torr
184.94918	11	Hg I		0.60	50×50	1.50-8.28
197.99565	12	Cu II	33	2.50	100×100	2.21-11.15
200.03459	12	Cu II	35	0.80	100×100	1.71-10.26
204.4458	12	Cu II	35	0.60	100×100	1.29-10.28
212.36503	10	Cu II	30	0.70	100×100	1.15-8.38
216.5775	12	Cu I	27	0.25	100×100	0.76-5.16
222.6391	12	Cu I	30	0.40	50×50	0.38-2.30
230.3826	15	Cu II	32	2.0	100×100	0.23-1.31
235.5735	11	Cu I	31	1.5	100×100	0.14-0.91
240.40687	13	Cu I	32	1.5	100×100	0.14-0.99
244.2378	6	Cu I	30	0.40	50×50	0.15-0.57
249.2898	11	Cu I	20	0.12	100×100	0.10-0.65

228K

λ nm	n	Line	I mA	T Sec	Slit μm	Pressure Torr
184.94918	12	Hg I		0.60	50×50	1.00-7.04
197.99565	10	Cu II	33	2.50	100×100	1.55-7.99
200.03459	12	Cu II	35	0.80	100×100	2.14-10.27
204.4458	9	Cu II	35	0.60	100×100	1.75-10.02
212.36503	11	Cu II	30	0.70	100×100	1.12-4.97
216.5775	9	Cu I	27	0.25	100×100	0.67-3.84
222.6391	13	Cu I	30	0.40	50×50	0.27-1.88
230.3826	16	Cu II	32	2.0	100×100	0.16-1.02
235.5735	12	Cu I	31	1.5	100×100	0.15-0.72
240.40687	11	Cu I	32	1.5	100×100	0.11-0.75
244.2378	9	Cu I	30	0.40	50×50	0.12-0.47
249.2898	10	Cu I	20	0.12	100×100	0.10-0.48

195K

λ nm	n	Line	I mA	T Sec	Slit μm	Pressure Torr
184.94918	11	Hg I		0.60	50×50	0.95-6.24
197.99565	12	Cu II	33	2.50	100×100	1.55-7.78
200.03459	12	Cu II	35	0.80	100×100	1.45-9.97
204.4458	12	Cu II	35	0.60	100×100	1.30-9.15
212.36503	12	Cu II	30	0.70	100×100	0.98-4.68
216.5775	12	Cu I	27	0.25	100×100	0.72-2.43
222.6391	9	Cu I	30	0.40	50×50	0.27-1.86
230.3826	17	Cu II	32	2.0	100×100	0.13-0.89
235.5735	11	Cu I	31	1.5	100×100	0.12-0.66
240.40687	13	Cu I	32	1.5	100×100	0.11-0.43
244.2378	9	Cu I	30	0.40	50×50	0.11-0.47
249.2898	11	Cu I	20	0.12	100×100	0.10-0.35

Table 2. Absorption cross sections of ozone, in unit of $10^{-x}cm^2$

λ, nm	x	Present*			Molina & Molina	
		295K	228K	195K	298K	226K
184.9	19	6.21[7]	6.23[6]	6.21[6]		
185.0	19				6.54	6.44
197.9	19	3.32[4]	3.32[6]	3.28[7]		
198.0	19				3.35	3.33
200.0	19	3.12[3]	3.04[4]	3.03[1]	3.15	3.15
204.4	19	3.31[5]	3.34[5]	3.35[3]		
204.5	19				3.47	3.49
212.3	19	7.31[2]	7.30[3]	7.34[3]		
216.5	18	1.18[1]	1.18[1]	1.19[2]	1.22	1.24
222.5	18				2.31	2.33
222.6	18	2.26[3]	2.33[4]	2.28[2]		
230.3	18	4.38[2]	4.43[3]	4.42[6]		
230.5	18				4.66	4.68
235.5	18	6.17[9]	6.18[5]	6.22[7]	6.45	6.48
240.4	18	7.98[8]	8.00[5]	8.02[6]		
240.5	18				8.40	8.42
244.0	18				9.72	9.75
244.2	18	9.42[6]	9.46[8]	9.51[6]		
244.5	18				9.75	9.78
249.2	17	1.07[2]	1.07[1]	1.07[1]		
249.5	17				1.112	1.121

*The numbers in the brackets are the estimated error of 1σ in the last digit.

The relative values are then normalized to the absolute cross sections that have been measured accurately at 12 wavelengths (Sec. 1.1). The cross sections of O_3 obtained and calibrated are presented in Fig. 1 of the attached preprint where open circles represent the absolute cross sections from measurements at atomic lines.

Temperature dependence of the cross sections of ozone are negligible. The absolute cross sections in Table 2 show that temperature variations of cross sections are within the experimental error and therefore we recommend to neglect temperature effects on the cross sections of ozone below 254 nm.

2. PUBLICATIONS

2.1 Paper Published and in Press

Absolute Absorption Cross Section Measurements of Ozone in the Wavelength Region 185-254 nm and the Temperature Dependence, K. Yoshino, J.R. Esmond, D.E. Freeman and W.H. Parkinson, J. Geophys. Res. submitted for publication.

2.2 Presentations during the period 10/1/89 - 5/31/92

High Resolution Spectroscopy and Stratrospheric Ozone Problems, Seminar at Institute of Atomic and Molecular Science, Academia Sinica, Taiwan, K. Yoshino, October 1990.

The Atmospheric Transmittance in UV and VUV Region, Seminar at National Institute for Environmental Studies, Tsukuba, Japan, K. Yoshino, November 1990.

The Atmospheric Transmittance in the vuv region, Seminar at The University of Tokyo, College of Arts and Science, K. Yoshino, November, 1991.

Absolute Absorption Cross Section Measurements of Ozone in the Wavelength Region 185-254 nm and the Temperature Dependence

K. Yoshino, J.R. Esmond, D.E. Freeman and W.H. Parkinson

Harvard-Smithsonian Center for Astrophysics

60 Garden Street, Cambridge, MA 02138, U.S.A.

Proofs to be mailed to: Dr. K. Yoshino
Harvard-Smithsonian Center for Astrophysics
60 Garden street, MS-50, Cambridge, MA 02138

Proposed Running Head: O_3 cross sections in the 185-254 nm

Pages: 10 (text, references and figure captions)

Figures: 2

Tables: 3

Abstract

Laboratory measurements of the relative absorption cross sections of ozone at the temperatures 195, 228 and 295 K have been made throughout the wavelength region 185—254 nm. The absolute absorption cross sections at the same temperatures have been measured at several discrete wavelengths in the region 185-250 nm. The absolute cross sections of ozone have been used to put relative cross sections on a firm absolute basis throughout the region 185—255 nm. These recalibrated cross sections are available as numerical compilations on magnetic tape from the National Space Science Data Center, NASA/Goddard Space Flight Center, Greenbelt, MD 20771, U.S.A.

1. INTRODUCTION

In the wavelength region 185-240 nm, the penetration of solar radiation into the Earth's atmosphere is controlled by O_2 and O_3, and the transmitted radiation is available to dissociate trace species. The Herzberg continuum absorption of O_2 has its photodissociation threshold at 242.2 nm, and its maximum cross section of only $\sim 7 \times 10^{-24}$ cm^2 occurs near 202 nm; below 202 nm the absorption cross section of O_2 increases rapidly with the onset of the predissociated Schumann-Runge bands. Coincidentally, the absorption minimum, $\sim 3 \times 10^{-19}$ cm^2, of O_3 occurs also near 202 nm, and the absorption by O_3 increases towards shorter and longer wavelengths. The ratio of the cross sections, $\sigma(O_3)/\sigma(O_2)$, approximately doubles for each 5 nm increase in wavelength between 205 and 240 nm, being about 5×10^4 at 205 nm and 8×10^6 at 240 nm. In the region 200-240 nm, both O_2 and O_3 play a joint critical role in atmospheric absorption, whereas O_3 becomes the principal absorber at 240-350 nm and O_2 at 100-200 nm.

The recommended cross sections of the World Meteorological Organization [WMO, 1986] were based on Tanaka et al. [1953] for the region 175-200 nm, and on Inn and Tanaka [1953] for the region 200-240 nm. In WMO [1986], it is stated that the results of Inn and Tanaka [1953] are supported by DeMore and Raper [1964] and by Griggs [1968]. In fact, near the minimum in the cross section at ~202 nm, the results of Inn and Tanaka are ~30% higher than those of Griggs; the results of DeMore and Raper are, on the average, systematically ~2% higher than those of Inn and Tanaka. The only cross section measurements below 240 nm published in the last twenty years are those of Molina and Molina [1986], and they give results at room temperature and at 226 K, an atmospherically significant temperature.

The aeronomic effects of the recent reductions in the Herzberg continuum absorption cross section of O_2 resulting from stratospheric [Anderson and Hall, 1983 and 1986] and laboratory [Cheung et al., 1986; Jenouvrier et al., 1986; Yoshino et al., 1988a] determinations have been studied by Nicolet and Kennes [1986], who also indicated the significance of uncertainties in the O_3 cross sections in the region 200-240 nm. They evaluated in detail the sensitivity of the stratospheric O_2 photodissociation rate to uncertainties in the most recent determinations of solar irradiances, O_2 cross sections, and O_3 cross sections. They concluded that uncertainties of 10% in the O_3 cross section in the region 202-242 nm are magnified into variations of up to 30% in the O_2 photolysis rate in the lower stratosphere. They stressed also that this rate is most sensitive to the absolute O_3 cross section in precisely the spectral interval (200-220 nm) where the differences between the laboratory measurements of the O_3 cross section by Inn and Tanaka [1953] and Molina and Molina [1986] are largest. Uncertainties in the O_3 cross sections are also propagated into uncertainties in the O_2 cross sections determined from in situ stratospheric measurements of the attenuation of solar or stellar radiation; for example, the O_2 cross sections obtained from the stratospheric measurements of Pirre et al. [1988] are reduced by amounts increasing from ~8% near 206 nm to 45% near 216 nm, as a result of using the O_3 cross sections of Molina and Molina instead of those of Inn and Tanaka.

We report here the results of the absolute cross section measurements of ozone at several discrete wavelengths in the region 185-254 nm at the temperatures 295, 228 and 195 K. We also obtained relative cross section measurements throughout the region 185-250 nm at these temperatures, and they have been put on an absolute scale using the measured absolute cross sections.

2. EXPERIMENTAL PROCEDURE

The general experimental arrangement has already been described in a previous paper [Yoshino et al., 1988b]. Ozone is prepared from pure oxygen (Airco grade 4.5 passed through a liquid nitrogen trap) at 78 K in a Tesla discharge, by collecting liquid ozone at 78 K. It is purified by pumping off residual oxygen from the oxygen/ozone mixture at 78 K. The absorption cell is directly connected to the exit slit assembly of a 0.3 m Czerny-Turner vacuum monochromator equipped with a 1600 line mm^{-1} grating. The instrumental width (FWHM) is 0.195 nm with entrance and exit slits widths of 0.10 mm. A Spacom integrated detector [Yoshino et al., 1980] with a EMR 541F photomultiplier is mounted at the other end of the absorption cell without further optical elements. The entire ozone column, with optical path length 10 cm, is cooled to 228 or 195 K by immersing the cell in stirred methanol which is cooled by a cold finger and controlled thermally within ±0.5 K. The hollow cathode or mercury lamps directly connected to the spectrometer are used as background line sources for the absolute cross section measurements at the selected wavelengths. In the scan mode, the background continuum is provided by a hydrogen discharge lamp, and a mercury lamp located behind the hydrogen lamp is used for wavelength calibration.

2.1 The measurements at fixed wavelengths.

The absolute absorption cross section of ozone at fixed wavelengths in the region 184-250 nm have been measured at 295 K, 228 K and 195 K. The 12 fixed wavelengths have been selected from atomic lines of Hg I, Cu I and Cu II. That the selected lines are free from any other lines within the resolution of the 0.3 m Czerny-Turner vacuum monochromator has been confirmed by high resolution spectra from our 6.65-m spectrograph. The mercury lamp with thermal control and a special Cu hollow cathode lamp provide suitable

atomic line sources. The absorption cross section of ozone in the wavelength region 185-250 nm varies from 1.15×10^{-17} to 3×10^{-19} cm^2. The optical depths measured were restricted to the range $\ln(I_0/I) \simeq 0.3-2.0$ to ensure good accuracy. With this restriction, the whole set of cross section measurements was performed with pressures of O_3 in the range 0.1—11 Torr.

2.2 The measurements in the wavelength region 185—254 nm.

Continuous cross sections of O_3 were measured in the wavelength region 180—245 nm with a hydrogen continuum as background source. A mercury lamp was also placed behind the hydrogen lamp and provided two Hg lines at 184.9 and 253.7 nm. These two Hg lines were used for wavelength calibration. Since wings of the strong Hg line at 253.7 nm overlapped the hydrogen continuum, some scans were taken without the Hg line at 253.7 nm. Scan speed was chosen as 7.5 nm/min with counting time 0.1 s which provided data points at every 0.0125 nm. The column density of O_3 was expected to vary during the scanning of the entire wavelength region because the VUV radiation destroys ozone molecules. Therefore the scan over an extended wavelength region was used to provide only continuous relative cross sections assuming the constant column density of O_3. The relative cross sections were then normalized to the absolute scale using the absolute cross sections measured at fixed wavelengths.

3. RESULTS AND DISCUSSION

The absolute cross sections of ozone have been measured at 12 wavelengths in the region 180—250 nm at 295 K, 228 K and 195 K, and they are listed in Table 1 where vacuum wavelengths are used. All measurements except the one at 184.9 nm were obtained with a Cu hollow cathode lamp. The 1% uncertainty in the cross section measurements arose mostly from the optical depth and column

density measurements. Another possible source of error is the purity of ozone which we assumed to be 100% pure to obtain the column density. If ozone is not pure, our measured cross sections will be lower limits as discussed in the previous paper [Yoshino et al., 1988b].

The cross sections of O_3 obtained in the scan mode at temperatures 295 K, 228 K, and 195 K are presented in Fig. 1 where open circles represent the absolute cross sections from measurements at atomic lines mentioned above. The cross sections at 195 K were extended toward longer wavelength with the previous high resolution data [Freeman et al., 1984; Yoshino et al., 1988b], which is recalibrated by the present absolute cross sections between 240 and 254 nm. Some weak structures around 250 nm are shown in the high resolution scan at 195 K, but these might be distorted in the low resolution scans at 228 K and 295 K. Analogous cross section data in numerical form are available for every 0.013 nm (2-4 cm^{-1}) by request. Cross sections for every 0.5 nm are given in Table 2 where cross sections of Molina and Molina [1986] are also presented for comparison. Our cross sections at room temperature are 2~5 % smaller than those of Molina and Molina [1986].

In atmospheric modeling, usage of the averaged cross sections over 500 cm^{-1} range has been standard, [WMO, 1986] and Table 3 presents such averaged cross sections of O_3 in 185-254 nm range along with those of Molina and Molina [1986] and WMO [1986]. Molina noticed that the largest discrepancy of 10% between WMO values and theirs occurs around 210 nm. WMO values are based on the results of Inn and Tanaka [1953; 1959] and their results agree with the later measurements by Griggs [1968]. Considering the relatively large experimental uncertainty of the old works, Molina and Molina concluded this was reasonable agreement. Averaged cross sections at 295 K in Table 3 are plotted in Fig. 2 against spectral interval (see Table 7-4 in WMO). WMO values represented by small dots are lower around the spectral interval 20 as

mentioned by Molina and Molina, but also they are high around the spectral interval 12. Our values, represented by a solid line, agree reasonably with those of Molina and Molina (broken line), but are slightly lower around the spectral interval 30. WMO values might show a slight shift due to the wavelength calibration around 200 nm region. Our values around 235 nm are lower than others but agree well in other wavelength regions.

The temperature dependences of the cross sections of ozone are negligible. The absolute cross sections in Table 1 show that temperature variations of cross sections are within the experimental error. Molecular absorption at the shorter wavelengths depends mostly on the transitions from the lowest ground vibrational levels. Therefore, temperature effects can be expected only from the variations of rotational populations with temperature, and they make very minor contributions to the total cross section. Below 254 nm, we recommend neglect of temperature effects on the cross sections of ozone within present experimental accuracy.

The new measurements of cross sections ozone below 250 nm are slightly lower than the those of Molina and Molina [1986]. As discussed in previous work [Yoshino et al., 1988b], the cross sections of Molina and Molina are always higher than any other results. Differences are within a few percent and would not be significant in atmospheric applications.

ACKNOWLEDGMENTS

This work reported was supported by the NASA Upper Atmospheric Research Program under Grant No. NAGW-1788 to the Smithsonian Astrophysical Observatory.

References:

Anderson, G.P. and L.A. Hall, Attenuation of Solar Irradiation in the Stratosphere: Spectrometer Results Between 191 and 207 nm, J. Geophys. Res. 88, 6801-6806, 1983.

Anderson, G.P. and L.A. Hall, Stratospheric Determination of O_2 Cross Sections and Photodissociation Rate Coefficients: 191-215 nm, J. Geophys. Res. 91, 14509-14514 1986.

Cheung, A.S.-C., K. Yoshino, W.H. Parkinson, S.L. Guberman, and D.E. Freeman, Absorption Cross Section Measurements of O_2 in the Wavelength Region 195-241 nm of the Herzberg Continuum, Planet. Space Sci. 34, 1007-1021, 1986.

DeMore, W.B. and O. Raper, Hartley Band Extinction Coefficients of Ozone in the Gas Phase and in Liquid Nitrogen, Carbon Monoxide, and Argon, J. Phys. Chem. 68, 412-414, 1964.

Freeman, D.E., K. Yoshino, J.R. Esmond, and W.H. Parkinson, High Resolution Absorption Cross Section Measurements of Ozone at 195 K in the Wavelength Region 240-350 nm, Planet. Space Sci. 32, 239-248, 1984.

Griggs, M., Absorption Coefficients of Ozone in the Ultraviolet and Visible Regions, J. Chem. Phys. 49, 857-859, 1968.

Inn, E.C. and Y. Tanaka, Absorption Coefficients of Ozone in the Ultraviolet and Visible Regions, J. Opt. Soc. Am. 43, 870-873, 1953.

Inn, E.C. and Y. Tanaka, Ozone Absorption Coefficients in the Visible and Ultraviolet Regions, Ozone Chemistry and Technology, Advances in Chemistry Series 21, 263-268, American chemical Society, Washington, D.C., 1959.

Jenouvrier, A., B. Coquart, and M.F. Merienne, Long Pathlength Measurements of Oxygen Absorption Cross Sections in the Wavelength Region 205-240 nm, J. Quant. Spectros. Radiat. Transfer 36, 349-354, 1986.

Molina, L.T. and M.J. Molina, Absolute Cross Sections of Ozone in the 185 to 350 nm Wavelength Range, J. Geophys. Res. 91, 14,501-14,507, 1986.

Nicolet, M. and R. Kennes, Aeronomic Problems of the Molecular Oxygen Photodissociation. I. The O_2 Herzberg Continuum, Planet. Space Sci. 36, 1043-1059, 1986.

Pirre, M., P. Rigaud, and D. Huguenin, In-Situ Measurements of the Absorption Cross-Sections of O_2 in the Herzberg Continuum: The Results of Two Different Experiments, Ann. Geophysicae 6, 535-540, 1988.

Tanaka, Y, E.C. Inn, and K. Watanabe, Absorption Coefficients of Gases in the Vacuum Ultraviolet. Part IV. Ozone, J. chem. Phys. 21, 1651-1653, 1953.

World Meteorological Organization, Atmospheric Ozone 1985, Global Ozone Research and Monitoring Project, Report No. 16, 1986.

Yoshino, K., D.E. Freeman, and W.H. Parkinson, Photoelectric Scanning (6.65 m) Spectrometer for VUV Cross-Section Measurements, Appl. Opt. 19, 66-71, 1980.

Yoshino, K., A.S.-C. Cheung, J.R. Esmond, W.H. Parkinson, D.E. Freeman, S.L. Guberman, A. Jenouvrier, B. Coquart, and M.F. Merienne, Improved Absorption Cross Sections of Oxygen in the Wavelength Region 205-240 nm of the Herzberg Continuum, Planet. Space Sci. 36, 1469-1475, 1988a.

Yoshino, K., D.E. Freeman, J.R. Esmond, and W.H. Parkinson, Absolute Absorption Cross-Section Measurements of Ozone in the Wavelength Region 238-335 nm and the Temperature Dependence, Planet. Space Sci. 36, 395-398, 1988b.

Figure Captions

Fig. 1. The cross sections of O_3 in the wavenumber range 39,000—54,000 cm^{-1}. Open circles are the absolute cross sections measured with Cu- and Hg-line sources. Cross sections at 195 K are extended to longer wavelengths using the previous values obtained with high resolution [Yoshino et al., 1988b].

Fig. 2. The averaged cross sections on the 500 cm^{-1} grid are plotted against the spectral interval (see Table 3 or Table 7-4 of WMO, 1986). Solid line refers to the present values, broken line to Molina and Molina [1986], and small dots to WMO [1986].

Table 1. Absolute Absorption Cross Sections of Ozone, in units of $10^{-x}cm^2$

Wavelength nm	Line	x	Cross Section 295K	228K	195K
184.94918	Hg I	19	6.21±0.07	6.23±0.06	6.21±0.06
197.99565	Cu II	19	3.32±0.04	3.32±0.06	3.28±0.07
200.03459	Cu II	19	3.12±0.03	3.04±0.04	3.03±0.01
204.4458	Cu II	19	3.31±0.05	3.34±0.05	3.35±0.03
212.36503	Cu II	19	7.31±0.02	7.30±0.03	7.34±0.03
216.5775	Cu I	19	11.84±0.08	11.82±0.09	11.94±0.15
222.6391	Cu I	18	2.26±0.03	2.33±0.04	2.28±0.02
230.3826	Cu II	18	4.38±0.02	4.43±0.03	4.42±0.06
235.5735	Cu I	18	6.17±0.09	6.18±0.05	6.22±0.07
240.40687	Cu I	18	7.98±0.08	8.00±0.05	8.02±0.06
244.2378	Cu I	18	9.42±0.06	9.46±0.08	9.51±0.06
249.2898	Cu I	18	10.70±0.22	10.70±0.12	10.69±0.13

Table 2. Absorption Cross Sections of O_3 between 185.0-253.5 nm at 0.5 nm Intervals (in units of 10^{-20} cm^2)

Wavelength	Present			Molina & Molina[a]		
nm	T=295K	T=228K	T=195K	T=298K	T=263K	T=226K
253.5	1143.	1158.	1134.	1155.	1155.	1167.
253.0	1104.	1131.	1108.	1140.	1142.	1149.
252.5	1110.	1119.	1098.	1139.	1137.	1143.
252.0	1125.	1142.	1154.	1155.	1153.	1165.
251.5	1108.	1112.	1127.	1146.	1153.	1164.
251.0	1086.	1085.	1078.	1114.	1115.	1123.
250.5	1080.	1070.	1087.	1113.	1110.	1118.
250.0	1090.	1086.	1103.	1124.	1121.	1134.
249.5	1052.	1070.	1073.	1112.	1110.	1121.
249.0	1053.	1069.	1080.	1112.	1110.	1124.
248.5	1054.	1048.	1047.	1082.	1082.	1094.
248.0	1042.	1031.	1045.	1071.	1072.	1079.
247.5	1029.	1026.	1035.	1068.	1069.	1080.
247.0	1000.	1002.	1009.	1047.	1051.	1058.
246.5	1000.	995.	1000.	1034.	1035.	1039.
246.0	993.	990.	1012.	1033.	1032.	1042.
245.5	971.	987.	992.	1025.	1028.	1040.
245.0	953.	950.	962.	993.	995.	1007.
244.5	948.	951.	947.	975.	971.	978.
244.0	941.	939.	951.	972.	968.	975.
243.5	927.	916.	931.	956.	957.	963.
243.0	899.	903.	907.	933.	932.	940.
242.5	882.	882.	883.	913.	911.	916.
242.0	855.	860.	872.	897.	895.	902.
241.5	832.	862.	851.	886.	886.	892.
241.0	818.	840.	829.	860.	859.	864.
240.5	805.	803.	805.	840.	838.	842.
240.0	798.	796.	791.	831.		837.
239.5	764.	772.	782.	810.		815.
239.0	738.	755.	755.	782.		784.
238.5	724.	736.	736.	768.		772.
238.0	715.	712.	718.	749.		753.
237.5	686.	686.	706.	728.		732.
237.0	669.	667.	684.	709.		714.
236.5	656.	657.	663.	690.		692.
236.0	644.	641.	645.	672.		677.
235.5	611.	616.	617.	645.		648.
235.0	601.	596.	611.	632.		635.
234.5	583.	586.	589.	615.		621.
234.0	559.	561.	569.	589.		592.
233.5	550.	551.	554.	572.		575.
233.0	530.	526.	534.	555.		559.
232.5	513.	518.	516.	537.		541.
232.0	492.	493.	505.	518.		523.
231.5	478.	477.	482.	498.		502.
231.0	456.	464.	463.	481.		486.
230.5	440.	443.	446.	466.		468.

230.0	423.	426.	428.	448.	451.
229.5	414.	411.	414.	432.	435.
229.0	397.	396.	402.	414.	416.
228.5	381.	379.	385.	398.	401.
228.0	366.	365.	368.	383.	386.
227.5	357.	349.	353.	367.	370.
227.0	340.	334.	338.	351.	354.
226.5	330.	330.	326.	337.	338.
226.0	312.	314.	310.	323.	324.
225.5	298.6	305.	296.1	308.	310.
225.0	288.3	292.0	285.4	294.3	296.3
224.5	276.3	277.0	273.3	280.9	282.8
224.0	261.8	265.8	261.9	268.4	268.8
223.5	247.8	258.3	250.5	254.8	257.2
223.0	236.0	244.7	236.7	242.9	244.3
222.5	222.9	231.6	224.6	231.2	232.6
222.0	210.5	219.0	214.6	220.0	221.7
221.5	201.6	208.4	206.7	209.0	210.3
221.0	190.2	194.7	193.4	198.2	200.0
220.5	180.3	184.3	185.8	188.8	190.0
220.0	174.4	173.6	175.9	178.5	179.9
219.5	163.4	164.7	167.0	169.4	171.8
219.0	155.1	155.3	157.1	160.1	163.8
218.5	145.7	146.8	148.3	152.0	154.8
218.0	139.8	137.2	141.5	143.9	146.4
217.5	131.7	130.3	132.5	136.2	138.7
217.0	124.8	122.0	125.4	128.7	131.4
216.5	117.3	116.3	118.2	121.5	124.1
216.0	110.5	109.4	111.2	114.6	116.9
215.5	106.0	102.1	105.3	108.1	110.4
215.0	98.6	96.4	99.2	102.3	104.1
214.5	93.4	91.5	93.6	96.4	98.3
214.0	87.6	86.1	87.6	91.0	92.6
213.5	83.9	81.6	83.2	85.7	87.5
213.0	78.4	77.4	79.5	81.0	82.6
212.5	73.9	74.5	74.7	76.4	78.0
212.0	69.7	69.0	69.0	71.9	73.1
211.5	66.0	65.3	65.2	68.0	69.0
211.0	63.2	62.3	62.1	64.0	69.0
210.5	59.5	58.8	58.0	60.6	61.7
210.0	55.7	55.2	55.5	57.2	58.1
209.5	53.4	52.1	52.4	54.1	54.9
209.0	50.9	49.3	49.4	51.2	54.9
208.5	48.3	46.5	47.4	48.8	49.4
208.0	46.0	44.8	44.3	46.4	46.8
207.5	43.7	43.1	42.5	44.2	44.5
207.0	41.4	41.8	40.6	42.0	42.4
206.5	39.6	39.1	38.7	40.1	40.7
206.0	37.3	37.7	37.1	38.6	38.9
205.5	36.0	36.0	35.9	37.1	37.4
205.0	34.7	35.3	34.1	35.9	36.2
204.5	33.5	33.8	33.4	34.7	34.9
204.0	32.9	32.8	32.2	33.7	34.0
203.5	32.7	31.6	31.4	33.2	33.3
203.0	31.6	31.8	30.9	32.5	32.6

202.5	30.9	30.9	30.6	32.1	31.8
202.0	29.9	30.5	30.6	31.8	31.6
201.5	30.2	30.1	29.39	31.6	31.5
201.0	31.3	30.4	29.37	31.2	31.3
200.5	30.5	30.1	29.51	31.5	31.6
200.0	31.5	30.3	30.2	31.5	31.5
199.5	31.0	30.8	30.4	31.8	31.5
199.0	30.6	31.9	31.8	32.1	32.1
198.5	31.4	32.5	32.1	32.8	32.5
198.0	33.2	33.4	32.5	33.5	33.3
197.5	32.3	34.4	33.6	34.4	34.0
197.0	34.1	34.8	33.5	35.0	34.6
196.5	34.4	35.9	35.1	35.6	35.5
196.0	37.1	36.0	36.1	36.7	36.4
195.5	36.0	37.1	36.9	37.7	37.2
195.0	36.8	38.7	37.9	38.6	38.3
194.5	39.7	39.9	39.0	40.1	39.8
194.0	39.5	41.0	40.2	40.7	40.9
193.5	41.0	42.5	41.2	42.1	42.2
193.0	42.6	43.2	43.6	43.4	43.1
192.5	43.0	44.6	44.1	44.9	44.6
192.0	44.3	46.1	45.3	46.1	46.0
191.5	45.9	46.7	46.3	47.4	47.1
191.0	47.8	47.9	47.9	48.8	48.4
190.5	47.4	48.8	49.1	49.9	49.9
190.0	50.1	49.3	50.4	51.1	51.6
189.5	51.5	50.9	50.6	53.2	52.6
189.0	52.9	52.9	52.1	54.2	54.6
188.5	54.9	53.3	53.0	56.1	56.1
188.0	55.9	54.9	54.1	56.6	56.6
187.5	55.8	56.6	56.0	59.0	59.1
187.0	58.0	58.3	56.4	59.4	59.3
186.5	59.2	59.9	57.9	61.3	61.7
186.0	60.5	60.3	59.1	61.9	62.6
185.5	61.3	60.2	60.6	63.8	63.2
185.0	62.0	61.6	62.3	65.4	64.4

[a]Molina and Molina [1986].

Table 3. Averaged absorption cross sections of ozone over the spectral intervals used in atmospheric model calculations in units of $10^{-x}cm^2$.

Spect. Interv.	Wavelength Range (nm)	x	Present Work 295K	Present Work 228K	Present Work 195K	WMO[a] 203/273K	Molina[b] 298K	Molina[b] 226K
7	185.185—186.916	19	6.02	6.00	5.91	6.40	6.22	6.23
8	186.916—188.679	19	5.61	5.57	5.47	5.88	5.76	5.76
9	188.679—190.476	19	5.17	5.11	5.07	5.31	5.26	5.26
10	190.476—192.308	19	4.70	4.69	4.68	4.80	4.77	4.75
11	192.308—194.175	19	4.19	4.23	4.22	4.38	4.29	4.27
12	194.175—196.078	19	3.86	3.81	3.75	4.11	3.85	3.82
13	196.078—198.020	19	3.49	3.48	3.41	3.69	3.49	3.46
14	198.020—200.000	19	3.26	3.17	3.13	3.30	3.24	3.22
15	200.000—202.020	19	3.27	3.02	2.97	3.26	3.15	3.14
16	202.020—204.082	19	3.37	3.19	3.12	3.26	3.26	3.27
17	204.082—206.186	19	3.65	3.55	3.48	3.51	3.63	3.65
18	206.186—208.333	19	4.25	4.21	4.17	4.11	4.33	4.37
19	208.333—210.526	19	5.31	5.21	5.18	4.84	5.39	5.46
20	210.526—212.766	19	6.71	6.71	6.69	6.26	6.93	7.05
21	212.766—215.054	19	8.73	8.61	8.76	8.57	9.03	9.20
22	215.054—217.391	18	1.13	1.12	1.14	1.17	1.18	1.20
23	217.391—219.780	18	1.46	1.48	1.50	1.52	1.54	1.57
24	219.780—222.222	18	1.91	1.96	1.95	1.97	1.99	2.00
25	222.222—224.719	18	2.44	2.54	2.49	2.55	2.55	2.57
26	224.719—227.273	18	3.04	3.15	3.12	3.24	3.22	3.24
27	227.273—229.885	18	3.82	3.82	3.87	4.00	4.01	4.04
28	229.885—232.558	18	4.72	4.69	4.72	4.83	4.90	4.94
29	232.558—235.294	18	5.63	5.60	5.68	5.79	5.90	5.93
30	235.294—238.095	18	6.53	6.60	6.70	6.86	6.97	7.01
31	238.095—240.964	18	7.65	7.75	7.76	7.97	8.07	8.11
32	240.964—243.902	18	8.68	8.84	8.89	9.00	9.15	9.20
33	243.902—246.914	18	9.66	9.73	9.80	10.00	10.09	10.18
34	246.914—250.000	17	1.06	1.05	1.05	1.08	1.09	1.10
35	250.000—253.165	17	1.12	1.11	1.13	1.13	1.13	1.14

[a]World Meteorological Organization [1986].
[b]Molina and Molina [1986].

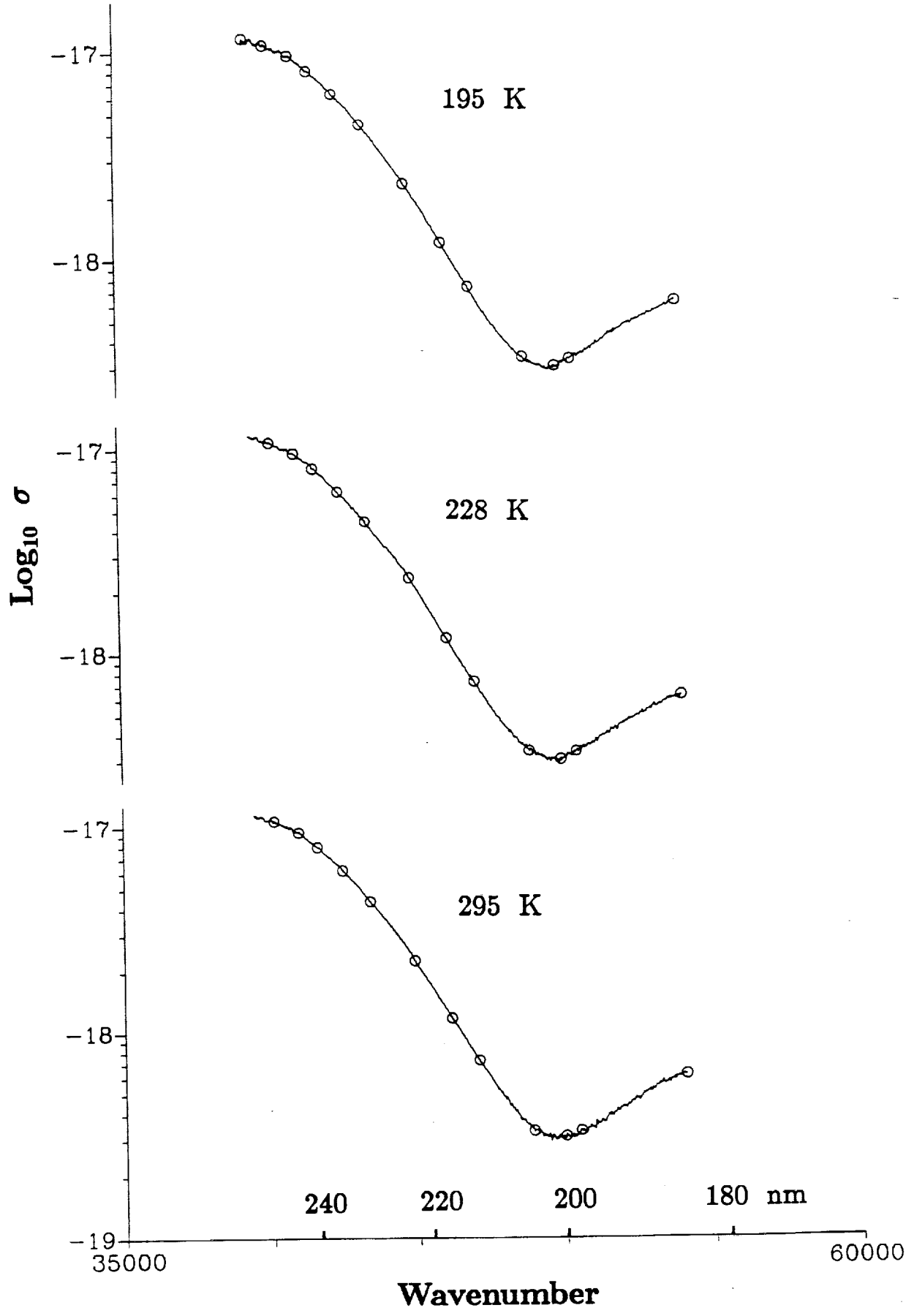
195 K
228 K
295 K
−17
−18
−19
Log10 σ
240
220
200
180 nm
35000
60000
Wavenumber

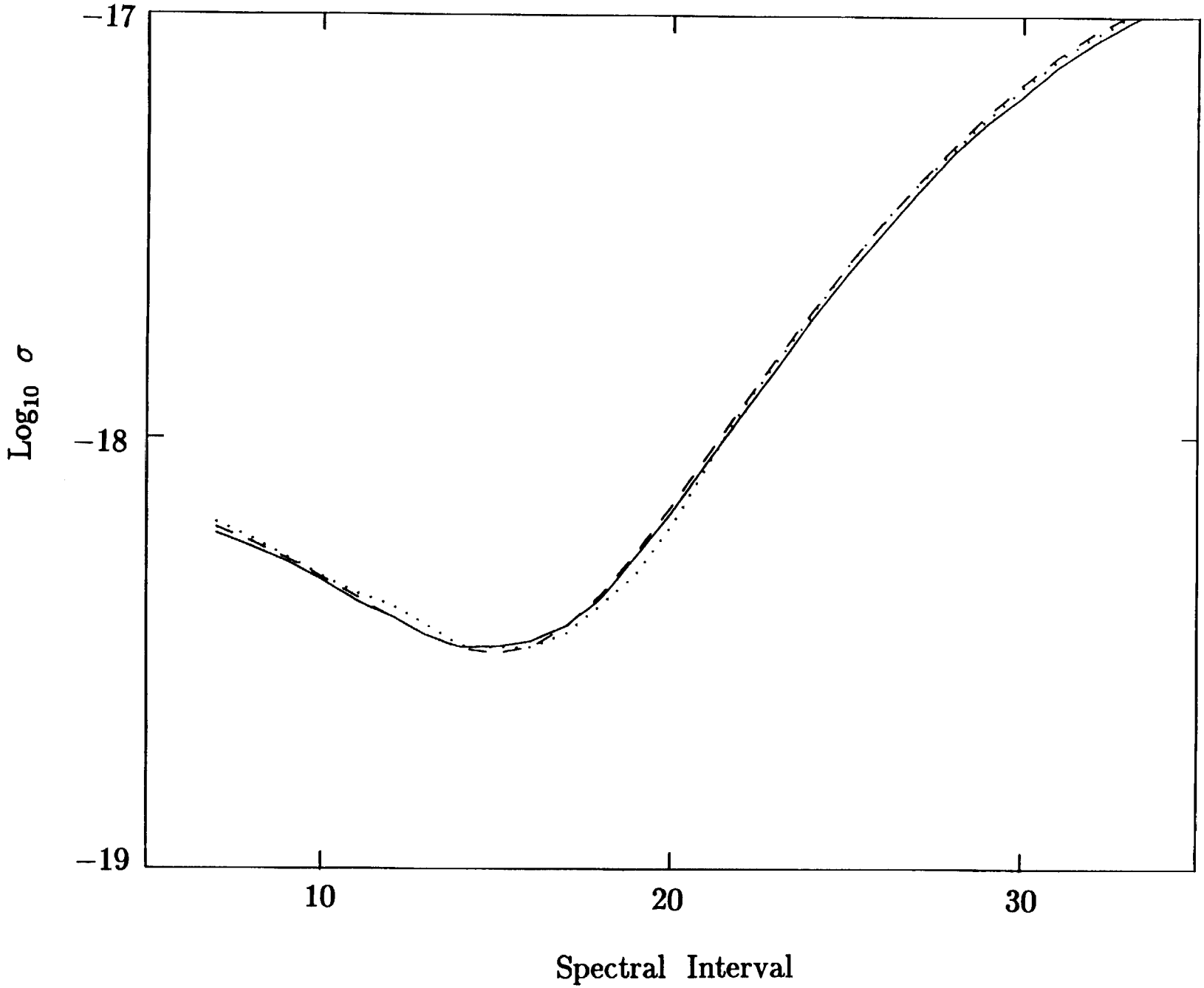
−17
−18
−19
Log10 σ
10
20
30
Spectral Interval